The confinement of Neptune's ring arcs by the moon Galatea

Fathi Namouni & Carolyn Porco

Southwest Research Institute, 1050 Walnut Street, Boulder, Colorado 80302, USA

Neptune has five narrow ring arcs, spanning about 40 degrees in longitude, which are apparently confined against the rapid azimuthal and radial spreading that normally results from inter-particle collisions. A gravitational resonance based on the vertical motion of the nearby neptunian moon Galatea was proposed[1,2] to explain the trapping of the ring particles into a sequence of arcs. But recent observations[3,4] have indicated that the arcs are away from the resonance, leaving their stability again unexplained. Here we report that a resonance based on Galatea's eccentricity is responsible for the angular confinement of the arcs. The mass of the arcs affects the precession of Galatea's eccentric orbit, which will enable a mass estimate from future observations of Galatea's eccentricity.

In the post-Voyager model[2], the moon Galatea produces a set of equilibrium points rotating at a constant rate (the pattern speed) that depends on the moon's mean motion and its vertical frequency about the planet's Laplace plane. However, as these corotation sites are potential maxima, dissipative inter-particle collisions tend to remove arc particles from the corotation sites, spreading the arcs azimuthally. Galatea can counterbalance the disruptive collisions by forcing the arc particles' orbits to be eccentric, thereby acting as an external source of energy. Before the recent observations, the arcs fell almost exactly at the location of the outer 86:84 corotation inclination resonance (CIR) of Galatea (Table 1, Fig. 1a,b) and within the 6 km width of its 43:42 Lindblad resonance (LR1) that forces the arc particle orbits to be eccentric. The 1998 observations of Neptune's arcs, however, yielded new mean motion measurements, $820.1122 \pm 0.0003 \deg \mathrm{d}^{-1}$ (ref. 5) and $820.1135 \pm 0.0009 \deg \mathrm{d}^{-1}$ (ref. 4) that differ from the previously inferred one $820.1185 \pm 0.0004 \deg \mathrm{d}^{-1}$ (refs 2, 6) by about $-5 \times 10^{-3} \deg \mathrm{d}^{-1}$, equivalent to an offset of 0.3 km. The new mean motion had in fact appeared previously in the data fits[6] obtained by combining ground-based and Voyager observations but was rejected in favour of the old value because the former displaces the arcs outside the CIR islands (Fig. 1c, d) where angular confinement is lost. A closer analysis of this offset shows that it cannot be accounted for by fine-tuning the system's parameters. More precisely, displacing the CIR from its current location by modifying Neptune's radius and quadrupole moment either implies large changes of order 25% in these parameters or introduces erroneous systematic offsets to the motion of Neptune's satellites. Alternatively, the CIR location can also be displaced by separately decreasing the regression rate of Galatea's mode under the action of a massive arc system. However, the required change, $-0.185 \deg \mathrm{d}^{-1}$, necessitates a mass at least ten

times larger than Galatea's. Finally, the CIR can be widened by increasing Galatea's mass; but in this case, the satellite must be at least three times more massive than the current estimate. This is inconsistent with the observed eccentric distortions forced on the arc system by Galatea[2].

The nearby corotation eccentricity resonance (CER) would be a candidate for the arcs' confinement were it not located 2 km inside the arcs' orbit (Table 1). The CER offers 43 potential maxima where arc particles can be trapped, with an angular extension of 8.37 deg, rotating at the pattern speed $n_{\mathrm{CER}} = n_{\mathrm{G}} - \kappa_{\mathrm{G}}/43 = 820.1481 \deg \mathrm{d}^{-1}$ where n_{G} and κ_{G} are, respectively, Galatea's mean motion and epicyclic frequency. The CER force, which is proportional to Galatea's eccentricity, e_{G}, will be stronger than the CIR, which is proportional to the square of Galatea's inclination, I_{G}. Both quantities are small: $I_{\mathrm{G}} = 0.0544 \pm 0.0132 \deg$ with respect to the invariable plane, and $e_{\mathrm{G}} = (0.120 \pm 0.149) \times 10^{-3}$ (ref. 7), though only I_{G} is measurably non-zero. It is possible to shift the CER exactly at the arcs' current location by accounting for the arcs' inertia, which has the effect of pulling on Galatea's apsidal line through the coupling of the CER to the Lindblad resonances LR1 and LR2 (Table 1). An estimate of the mass of the ring that would be required to switch on the resonance can be obtained from the condition that the CER angle is stationary. Exact resonance requires that the mismatch between the arcs' current mean motion[5], $n = 820.1122 \deg \mathrm{d}^{-1}$, and the CER pattern speed, n_{CER}, equal the precession rate of Galatea's pericentre induced by the massive ring and denoted $\varpi_{\mathrm{G,ring}}$:

$$\varpi_{\mathrm{G,ring}} = 43(n - n_{\mathrm{CER}}) \tag{1}$$

Three main effects contribute to $\varpi_{\mathrm{G,ring}}$: first, the CER as the strongest of the three induces a regression of Galatea's pericentre given by:

$$\varpi_{\mathrm{G,CER}} = m\alpha M^{-1} f_{\mathrm{CER}}(\alpha) n_{\mathrm{G}} e_{\mathrm{G}}^{-1} \tag{2}$$

when m is the ring's mass, M is Neptune's mass, $\alpha = 0.9844$ is the semi-major axes ratio of Galatea and the arcs, $f_{\mathrm{CER}}(0.9844) = -35.65$ is the CER strength evaluated with the observed semi-major axes, and $n_{\mathrm{G}} = 839.6615 \deg \mathrm{d}^{-1}$ (ref. 5) is Galatea's mean motion. Second, the LR2 also contributes a regression of Galatea's pericentre given by:

$$\varpi_{\mathrm{G,LR2}} = m\alpha M^{-1} f_{\mathrm{LR2}}(\alpha) n_{\mathrm{G}} e e_{\mathrm{G}}^{-1} \tag{3}$$

where $f_{\mathrm{LR2}}(0.9844) = -5941.82$ is the LR2 strength. Third, the secular potential that arises from the averaged motion of Galatea and the ring causes a precession of the satellite's pericentre given by:

$$\varpi_{\mathrm{G,sec}} = (2\pi)^{-1} m\alpha M^{-1} n_{\mathrm{G}} (1 - \alpha)^{-2} \tag{4}$$

Substituting equations (2)–(4) into equation (1), the ring's mass is given by:

$$m = \frac{43(n - n_{\mathrm{CER}}) M e_{\mathrm{G}}}{n_{\mathrm{G}} \alpha (f_{\mathrm{CER}} + f_{\mathrm{LR2}} e + (2\pi)^{-1}(1 - \alpha)^{-2} e_{\mathrm{G}})} \tag{5}$$

This relation implies that for a given ring mass and satellite eccentricity, arcs can be stabilized in resonance over a continuum of semi-major axes (Fig. 2). The current uncertainty in Galatea's eccentricity allows a wide range of masses for the ring system: from $0.23\, m_{\mathrm{G}}$ where $m_{\mathrm{G}} = 2.1 \times 10^{21}$ g is Galatea's mass for $e_{\mathrm{G}} = 10^{-4}$, to $0.002\, m_{\mathrm{G}}$ for $e_{\mathrm{G}} = 10^{-6}$. However, as the resonance width, W_{CER}, is related to e_{G} through $W_{\mathrm{CER}} = 2.5(e_{\mathrm{G}}/10^{-4})^{1/2}$ km, the arcs' current semi-major axis width, W_{arc}, can provide a constraint on Galatea's eccentricity and therefore the ring's mass by equating W_{arc} and W_{CER}. Unfortunately, the arcs' true spread in semi-major axis is poorly known. We choose the nominal value $W_{\mathrm{arc}} = 0.4$ km corresponding to that of the CIR resonance model and the corresponding kinematic fit[2]. This yields $e_{\mathrm{G}} = 2.5 \times 10^{-6}$ and a ring mass of 0.006 m_{G}. In Fig. 1e, f, a particle of mass 0.002 m_{G} is shown to librate in the 43:42 CER for $e_{\mathrm{G}} = 10^{-6}$—a detailed analysis (F.N. and C.P., to

Table 1 Galatea's resonances

Resonance type	Resonance angle	Δa (km)
Eccentric corotation	$43\lambda - 42\lambda_{\mathrm{G}} - \varpi_{\mathrm{G}}$	−1.99
Lindblad 2	$86\lambda - 84\lambda_{\mathrm{G}} - \varpi_{\mathrm{G}} - \varpi$	−1.97
Lindblad 1	$43\lambda - 42\lambda_{\mathrm{G}} - \varpi$	−1.94
Parametric	$86\lambda - 84\lambda_{\mathrm{G}} - 2\Omega$	−0.33
Vertical	$86\lambda - 84\lambda_{\mathrm{G}} - \Omega_{\mathrm{G}} - \Omega$	−0.31
Inclined corotation	$86\lambda - 84\lambda_{\mathrm{G}} - 2\Omega_{\mathrm{G}}$	−0.29

Shown are the inventory of resonances associated with Galatea in the arcs' neighbourhood. The resonance distance to the arcs, Δa, is referred to the new location[5] 62,932.85 km and has been shifted by +0.15 km to account for the synodic change in mean motion that is due to Galatea's action on the ring-particle[14]. The variables λ, ϖ, Ω, λ_{G}, ϖ_{G}, Ω_{G} are respectively the mean longitude, the longitude of the pericentre and the longitude of the ascending node of a ring-particle and Galatea.
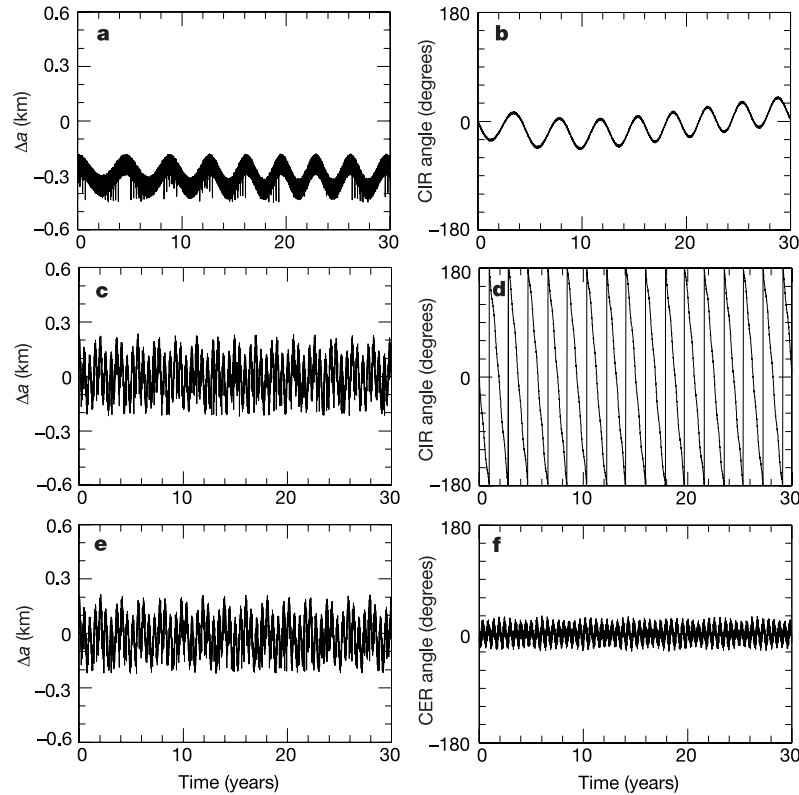
Figure 1 The motions of arc particles around Neptune. Numerical integration of the motion of an arc particle interacting with Galatea (mass 2.1×10^{21} g, eccentricity 10^{-6}, inclination 0.052 deg, mean motion[5] 839.6615 deg d^{-1}, corresponding to a geometric semi-major axis of 61,952.60 km). **a**, **c**, **e**, Δa denotes the geometric semi-major axis of the arc particle referred to the location given by the latest set of observations according to ref. 5, 62,932.85 km. **b**, **d**, **f**, The corotation inclination and eccentricity resonance (CIR and CER) angles are respectively $86\lambda - 84\lambda_G - 2\Omega_G - 180$ deg and $43\lambda - 42\lambda_G - \varpi_G$. **a**, **b**, The old model of angular confinement of the CIR of width 0.45 km. The arcs were thought to be 0.3 km closer to Galatea than the latest observations indicate. The libration of the CIR angle ensures that the collective motion of

the arc particles has the appearance of an arc centred on the corotation equilibrium site. **c**, **d**, The revised evolution of the arcs after the new observations put the arcs 0.3 km outside the location of the CIR. In this case the CIR angle is circulating through 360 deg and angular confinement is lost. **e**, **f**, The evolution of a massive arc system with mass ratio to Galatea of 0.002 and located at the arcs' current position. In this case the CER angle librates around 0 deg, ensuring confinement. In addition, the vertical resonance that is almost coincident with the CIR (Table 1) forces a small inclination, 0.019 deg, on the arcs with respect to Neptune's invariable plane[15]. This value differs from the provisional Voyager value of 0.062 deg which is more likely to be due to errors in identifying the orientation of Neptune's pole[2,6].

be published elsewhere) shows that the previous formulae over-estimate the arcs' mass. Decreasing the arcs' mass below the threshold value results in the increase of the CER libration amplitude until the arc particle is no longer librating. Unlike the CIR, the CER can be shifted easily to the arcs' position because the pericentre regression rate it forces on Galatea is proportional to e_G^{-1} which can be large even for a small mass ring. The CIR-induced nodal regression rate on the other hand scales as $II_G^{-1} \approx 1$ resulting in a negligible shift of the resonance location.

The angular confinement by the CER can now explain the angular length of the arc Fraternité[8], approximately 10 deg, as the result of occupying a single corotation site. This feature remained unexplained in the CIR model because the arc was found to extend over 2 to 3 consecutive corotation sites of width 4.18 deg despite the presence of unstable equilibria within it. This observation, together with the inability of the CIR to be shifted substantially from its nominal location, raises the question: is the CIR effect needed at all to explain the arc structure? The answer lies in the spacings of some of the smaller arcs[8]: the location of arc Égalité 2, of length about 3 deg, 10 deg away from the centre of Fraternité, and 3 deg away from the centre of Égalité 1, of length about 1 deg, does not match the 8.37-deg spacings of the CER. However, the coupling of the CIR and CER potentials at the current location modifies the shape of the CER potential by introducing additional equilibria with smaller
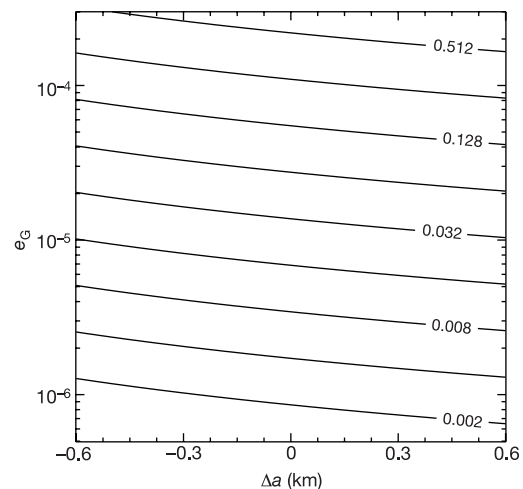

Figure 2 The effect of ring mass on the resonance location. The ring's mass required to shift the 43:42 corotation eccentricity resonance (CER), scaled to Galatea's mass 2.1×10^{21} g, is given by the level curves of equation (5) as a function of the semi-major axis referred to the current position of the arcs Δa, and Galatea's eccentricity e_G. As equation (5) is approximately linear as a function of the eccentricity, a small arc mass is sufficient to shift the CER.

spacings that match the observation of the smaller arcs. Conversely, we note that if the arcs' current mean motion did not differ from that of the CIR, that is, if there were no observed offset, the CER is still the only resonance that can both confine the arcs and explain the longer radial structures; the required mass for shifting the CER to the CIR location can be found in Fig. 2.

The ring mass we determined, $0.002m_G$ assuming $e_G = 10^{-6}$, corresponds to a parent 10-km-radius satellite with a density similar to Galatea's. We note that many of our results can be reproduced in the case of a massless arc system if a second satellite shares its orbit. A similar model was put forward shortly after the discovery of the ring arc system but prior to Voyager's more detailed observations[16]. A closer inspection of this two-satellite model however shows that the second satellite would produce a single continuous arc at each equilibrium point (L_4 or L_5), leaving the sequence of small arcs unexplained. A satellite co-orbital to the arcs of mass $0.002m_G$ would activate the CER, which in turn modifies the satellite's potential near L_4 and L_5 to allow a structure similar to the arcs. However, Voyager data exclude[9] undetected satellites of radius larger than 6 km implying that the mass required for the angular confinement of the arcs is not contained in a single body. Modelling the breakup of an arc parent satellite[10,11] should henceforth include the dynamical effects described in this paper in order to ascertain the angular distribution of mass and solve the problem of radial stability of the arcs. If the torques exerted by Galatea on the arcs work like those in Saturn's rings[12,13], the rate of radial migration of the arcs is $2.4\,\mathrm{km\,yr^{-1}}$, disrupting the arcs in less than a year. However, the satellite's torque is less likely to cause a significant drift in the arcs' radial position if the rings' mass is concentrated in a few clumps.

The value estimated here for Galatea's eccentricity, about 10^{-6}, is consistent with the requirement that the arcs have a small mass, regardless of the physical model responsible for their angular confinement. The fact that the current spread in semi-major axis of the arcs leads to such a small eccentricity is encouraging, because we expect that the decay timescale of Galatea's eccentricity due to the tides raised by Neptune[1] is of the order of 10^8 years, implying a rapid circularization of the orbit over the age of the Solar System. More precise measurements of Galatea's orbital elements, as well as models of the tidal evolution of the inner neptunian satellites together with the ring–Galatea interaction[13], are needed to fully validate the resonance model presented here and determine the origin of the small residual eccentricity in Galatea's orbit responsible for the arcs' confinement. ☐

1. Goldreich, P., Tremaine, S. & Borderies, N. Towards a theory for Neptune's arc rings. *Astron. J.* **92**, 490–494 (1986).
2. Porco, C. An explanation for Neptune's ring arcs. *Science* **400**, 995–1001 (1991).
3. Dumas, C. *et al.* Stability of Neptune's arcs in question. *Nature* **400**, 733–735 (1999).
4. Sicardy, B. *et al.* Images of Neptune's ring arcs obtained by a ground-based telescope. *Nature* **400**, 731–733 (1999).
5. Dumas, C. *et al.* Astrometry and near infra-red photometry of Neptune's inner satellites and ring arcs. *Astron. J.* (in the press).
6. Nicholson, P. D., Mosquiera, I. & Matthews, K. Stellar occultation observations of Neptune's rings: 1984–1988. *Icarus* **113**, 295–330 (1995).
7. Owen, W. M., Vaughan, R. M. & Synnott, S. P. Orbits of the six new satellites of Neptune. *Astron. J.* **101**, 1511–1515 (1991).
8. Porco, C. *et al.* in *Neptune and Triton* (ed. Cruikshank, D. P.) 703–804 (Univ. Arizona Press, Tucson, 1995).
9. Smith, B. A. *et al.* Voyager 2 and Neptune: Imaging science results. *Science* **246**, 1422–1449 (1989).
10. Colwell, J. E. & Esposito, L. W. A model for dust production for Neptune's ring system. *Geophys. Res. Lett.* **17**, 1741–1744 (1990).
11. Colwell, J. E. & Esposito, L. W. Origin of the rings of Neptune and Uranus: II Initial conditions and ring moon population. *J. Geophys. Res.* **98**, 7387–7401 (1993).
12. Goldreich, P. & Tremaine, S. The dynamics of planetary rings. *Annu. Rev. Astron. Astrophys.* **20**, 249–283 (1982).
13. Namouni, F. Ringlet-satellite interactions. *Mon. Not. R. Astron. Soc.* **300**, 915–930 (1998).
14. Horanyi, M. & Porco, C. Where exactly are the arcs of Neptune? *Icarus* **106**, 525–535 (1993).
15. Hänninen, J. & Porco, C. Collisional simulations of Neptune's ring arcs. *Icarus* **126**, 1–27 (1997).
16. Lissauer, J. J. Shepherding model for Neptune's arc ring. *Nature* **318**, 544–545 (1985).

Competing interests statement
The authors declare that they have no competing financial interests.

Correspondence and requests for materials should be addressed to F.N. (e-mail: fathi@ciclops.swri.edu).

••

Towards Bose–Einstein condensation of excitons in potential traps

L. V. Butov*, C. W. Lai*, A. L. Ivanov†, A. C. Gossard‡ & D. S. Chemla*§

* *Materials Sciences Division, E. O. Lawrence Berkeley National Laboratory;*
§ *Department of Physics, University of California at Berkeley, Berkeley, California 94720, USA*
† *Department of Physics and Astronomy, Cardiff University, Cardiff CF24 3YB, UK*
‡ *Department of Electrical and Computer Engineering, University of California, Santa Barbara, California 93106, USA*

An exciton is an electron–hole bound pair in a semiconductor. In the low-density limit, it is a composite Bose quasi-particle, akin to the hydrogen atom[1]. Just as in dilute atomic gases[2,3], reducing the temperature or increasing the exciton density increases the occupation numbers of the low-energy states leading to quantum degeneracy and eventually to Bose–Einstein condensation (BEC)[1]. Because the exciton mass is small—even smaller than the free electron mass—exciton BEC should occur at temperatures of about 1 K, many orders of magnitude higher than for atoms. However, it is in practice difficult to reach BEC conditions, as the temperature of excitons can considerably exceed that of the semiconductor lattice. The search for exciton BEC has concentrated on long-lived excitons: the exciton lifetime against electron–hole recombination therefore should exceed the characteristic timescale for the cooling of initially hot photo-generated excitons[4–10]. Until now, all experiments on atom condensation were performed on atomic gases confined in the potential traps. Inspired by these experiments, and using specially designed semiconductor nanostructures, we have collected quasi-two-dimensional excitons in an in-plane potential trap. Our photoluminescence measurements show that the quasi-two-dimensional excitons indeed condense at the bottom of the traps, giving rise to a statistically degenerate Bose gas.

More than three decades ago Keldysh and Kozlov[1] showed that in the dilute limit, $na_B^D \ll 1$ (a_B is the exciton Bohr radius, n the exciton density and D the dimensionality), excitons behave as weakly interacting Bose particles and are expected to undergo the Bose–Einstein condensation (BEC). Because the exciton mass, M, is very small, the three-dimensional critical temperature for exciton BEC, $T_c^{3D} = 0.527k_B^{-1}2\pi\hbar^2M^{-1}(n/g)^{2/3}$ (g is the spin degeneracy of the exciton state, k_B is the Boltzmann constant), should reach several Kelvins at experimentally accessible exciton densities, that is, about six orders of magnitude higher than the critical temperature for atom BEC. The theoretical predictions for exciton BEC and